THE JOURNAL OF BIOLOGICAL CHEMISTRY VOL. 283, NO. 10, pp. 6489–6500, March 7, 2008

RNA-binding Protein TLS Is a Major Nuclear Aggregate-interacting Protein in Huntingtin Exon 1 with Expanded Polyglutamine-expressing Cells*

Received for publication, June 28, 2007, and in revised form, December 27, 2007 Published, JBC Papers in Press, December 31, 2007, DOI 10.1074/jbc.M705306200

Hiroshi Doi[‡§], Kazumasa Okamura[‡], Peter O. Bauer[‡], Yoshiaki Furukawa[‡], Hideaki Shimizu[‡], Masaru Kurosawa[‡], Yoko Machida[‡], Haruko Miyazaki[‡], Kenichi Mitsui[¶], Yoshiyuki Kuroiwa[§], and Nobuyuki Nukina[‡1]

From the [‡]Laboratory for Structural Neuropathology and the [¶]Reseach Resource Center, RIKEN Brain Science Institute, 2-1 Hirosawa Wako-shi, Saitama, 351-0198, Japan and the [§]Department of Neurology, Graduate School of Medicine, Yokohama City University, 3-1, Fukuura, Kanazawa-ku, Yokohama 236-0004, Japan

Formation of intracellular aggregates is the hallmark of polyglutamine (polyQ) diseases. We analyzed the components of purified nuclear polyQ aggregates by mass spectrometry. As a result, we found that the RNA-binding protein translocated in liposarcoma (TLS) was one of the major components of nuclear polyQ aggregate-interacting proteins in a Huntington disease cell model and was also associated with neuronal intranuclear inclusions of R6/2 mice. *In vitro* study revealed that TLS could directly bind to truncated N-terminal huntingtin (tNhtt) aggregates but could not bind to monomer GST-tNhtt with 18, 42, or 62Q, indicating that the tNhtt protein acquired the ability to sequester TLS after forming aggregates. Thioflavin T assay and electron microscopic study further supported the idea that TLS bound to tNhtt-42Q aggregates at the early stage of tNhtt-42Q amyloid formation. Immunohistochemistry showed that TLS was associated with neuronal intranuclear inclusions of Huntington disease human brain. Because TLS has a variety of functional roles, the sequestration of TLS to polyQ aggregates may play a role in diverse pathological changes in the brains of patients with polyQ diseases.

Huntington disease (HD)[2] is a hereditary neurodegenerative disease caused by an expansion of the CAG repeat located in exon 1 of the HD gene (1). Expansion of the polyglutamine (polyQ) stretch in huntingtin (htt), the HD gene product, leads to the formation of intracellular aggregates (2, 3). Previous studies have demonstrated that nuclear accumulation of insoluble polyQ aggregates or formation of neuronal intranuclear inclusions is closely correlated with disease progression (4–6), and disruption of nuclear physiological processes may account for many of the disease phenotypes in the mouse models generated by expressing mutant N-terminal fragments of htt (7).

There are many aggregate-interacting proteins (AIPs), some of which, including the heat shock protein (Hsp) 40, 70, and 90 families, are thought to suppress aggregate formation and cellular toxicity induced by expanded polyQ proteins (8, 9). In addition, functionally important proteins, including transcription factors (10–12) and members of the ubiquitin-proteosome pathway (13, 14), are sequestered in the polyQ aggregates, which could cause their loss of function and result in cellular dysfunction. These studies suggest that the components of AIPs reflect either the cellular defense against polyQ aggregates or the cellular machinery affected by polyQ aggregates. Therefore, identification of AIPs should help elucidate the process of aggregate formation, the cellular response to aggregates, and the mechanisms of cellular dysfunction caused by the polyQ aggregates, but the AIPs are still not fully uncovered.

We have previously established a method to identify the components of nuclear polyQ AIPs from Neuro2a cells stably transfected with tNhtt-150Q-EGFP-NLS (HD150Q-NLS cells), which express a cDNA encoding htt exon 1 containing 150 CAG repeats and fused with enhanced green fluorescent protein (EGFP) and nuclear localization signals (NLS) (15). Using this method, we identified ubiquitin-interacting proteins, ubiquilin 1,2 and Tollip, as new AIPs and confirmed that the method was applicable to the analysis of AIPs.

In this report, we extended our previous study and found that the RNA-binding protein TLS (translocated in liposarcoma) (16), also known as FUS (17), is the major component of nuclear polyQ aggregates, and its family proteins, EWS and TAF15, are also found in purified polyQ aggregates. TLS is associated with polyQ aggregates formed by tNhtt-150Q-EGFP-NLS and ataxin-3 with 130Q in Neuro2a and HeLa cells, and neuronal intranuclear inclusions (NIIs) in a mouse model of HD. In an *in vitro* assay, we showed that TLS can directly bind to polyQ aggregates in the early stage of amyloid formation but cannot bind to monomer GST-tNhtt fusion proteins with 18, 42, or 62Q, suggesting that TLS is sequestered to polyQ aggregates through the conformational change of expanded polyQ stretches.

* This work was supported in part by grants-in-aid from the Ministry of Health, Labor and Welfare and the Ministry of Education, Culture, Sports, Science and Technology of Japan. The costs of publication of this article were defrayed in part by the payment of page charges. This article must therefore be hereby marked "*advertisement*" in accordance with 18 U.S.C. Section 1734 solely to indicate this fact.

[1] To whom correspondence should be addressed: 2-1 Hirosawa Wako-shi, Saitama, 351-0198, Japan. Fax: 8148-462-4796; E-mail: nukina@brain.riken.jp.

[2] The abbreviations used are: HD, Huntington disease; polyQ, polyglutamine; tNhtt; truncated N-terminal huntingtin; AIP, aggregate-interacting protein; EGFP, enhanced green fluorescent protein; NLS, nuclear localization signal; NII, neuronal nuclear inclusion; HRP, horseradish peroxidase; TBP, TATA-binding protein; TLS, translocated in liposarcoma; dbcAMP, N^6,2′-*O*-dibutyryl cyclic AMP; PBS, phosphate-buffered saline; siRNA, small interfering RNA; PVDF, polyvinylidene difluoride; GST, glutathione S-transferase; CBP, cyclic AMP-responsive element-binding protein-binding protein; Ab, antibody.

EXPERIMENTAL PROCEDURES

Mice—Heterozygous htt exon 1 transgenic male mice of the R6/2 (145 CAG repeats) strain (Jackson code, B6CBA-TgN (HD exon 1) 62) were obtained from Jackson Laboratory (Bar Harbor, ME). R6/2 mice and their age-matched controls were sacrificed, and their brains were collected. The mouse experiments were approved by the animal experiment committee of the RIKEN Brain Science Institute.

Antibodies—Polyclonal antibodies were generated in rabbits against the following peptides. Anti-TLS antibodies Ab-TLS-M and Ab-TLS-C were generated against amino acids 260–274 and 501–518 of mouse TLS, respectively. An anti-EWS antibody, Ab-EWS-M, was generated against amino acids 349–363 of mouse EWS. Anti-TAF15 antibodies Ab-TAF15-M and Ab-TAF15-C were generated against amino acids 155–173 and 541–554 of mouse TAF15, respectively. An N- or a C-terminal cysteine residue was added to each peptide for coupling to keyhole limpet hemocyanin or to SulfoLink Coupling Gel (Pierce). These polyclonal antibodies were affinity-purified using the SulfoLink kit (Pierce Biotechnology). Monoclonal anti-htt (EM48; MAB5374), monoclonal anti-polyglutamine (1C2; MAB1574), and monoclonal anti-ubiquitin (MAB1510) were from Chemicon International (Temecula, CA); monoclonal anti-GFP (clones 7.1 and 13.1) was from Roche Applied Sciences; monoclonal anti-v5 (R960-25) and horseradish peroxidase (HRP)-conjugated anti-v5 (R961-25) were from Invitrogen; monoclonal anti-Hsp70 (SPA-810) was from Stressgen Biotechnologies (Victoria, Canada); and rabbit polyclonal anti-TATA-binding protein (TBP) (SC-204), goat polyclonal anti-EWS (Ab-EWS-C; SC-6532), and anti-lamin B (SC-6217) were from Santa Cruz Biotechnology (Santa Cruz, CA). HRP-conjugated anti-mouse IgG (NA931V) and anti-rabbit IgG (NA934V) were from Amersham Biosciences; and HRP-conjugated anti-goat IgG (#705-035-147) was from Jackson ImmunoResearch Laboratories (West Grove, PA). Anti-mouse IgG conjugated with Alexa-546 (A-11030) and anti-rabbit IgG conjugated with Alexa-488 (A-11008) were from Molecular Probes (Eugene, OR).

Cell Culture—Neuro2a cell line stably transfected with tNhtt-150Q-EGFP-NLS (HD150Q-NLS cells), which express a cDNA encoding htt exon 1 containing 150 CAG repeats and fused with EGFP and NLS (15), were previously established using the ecdysone-inducible mammalian expression system (Invitrogen) (18, 19). Neuro2a cells, HD150Q-NLS cells, and HeLa cells were maintained in Dulbecco's modified Eagle's medium (Invitrogen) supplemented with 10% fetal bovine serum and penicillin-streptomycin (Invitrogen) at 37 °C in an atmosphere containing 5% CO_2. To differentiate the Neuro2a cells, N^6,2′-*O*-dibutyryl cyclic AMP (dbcAMP; Nacalai Tesque, Kyoto, Japan) was added to the medium, and to induce the expression of the tNhtt-polyQ-EGFP-NLS proteins, ponasterone A (Invitrogen) was added. To isolate nuclear aggregates or to prepare a nuclear soluble fraction, HD150Q-NLS cells were plated in 150-mm dishes and cultured overnight. The medium was supplemented with 5 mM dbcAMP or with both 5 mM dbcAMP and 1 μM ponasterone A. After 3 days, the cells were washed twice with ice-cold phosphate-buffered saline (PBS) and collected by centrifugation at 1000 rpm for 5 min. HD150Q-NLS cells treated with 5 mM dbcAMP were designated HD150Q-NLS-D cells, and HD150Q-NLS cells treated with both 5 mM dbcAMP and 1 μM ponasterone A were designated HD150Q-NLS-D/I cells.

Transfection of Plasmids and siRNA—cDNA for mouse TLS, EWS, and TAF15 were obtained by reverse transcription-PCR from the total RNA fraction of adult mouse brain. Each PCR product amplified from cDNA was subcloned into TOPO-pcDNA3.1-v5/His mammalian expression vector (Invitrogen). To make TLS deletion mutants, each deletion fragment indicated in the figure was amplified from pcDNA3.1-TLS-v5/His and was subcloned into TOPO-pcDNA3.1-v5/His. For the N-terminal deletions, the sequence AGCCACCATG was added to the 5′ end of each fragment. To make pcDNA3.1-tNhtt-polyQ (17Q or 153Q)-EGFP-NLS, tNhtt-polyQ-EGFP-NLS fragments were cut from pIND-tNhtt-polyQ-EGFP-NLS (19) with HindIII-XbaI digestion, and the resulting fragments were inserted into pcDNA3.1-v5/His. All of the constructs were verified by DNA sequencing. Transfection of each plasmid into the cells was performed using Lipofectamine 2000 reagent (Invitrogen).

siRNA for TLS (siRNA ID 88406) was purchased from Ambion, Inc. (Austin, TX). siRNA for luciferase (D-001100-01-20) was purchased from Dharmacon, Inc. (Lafayette, CO). siRNAs were mixed at the indicated concentrations and transfected using Lipofectamine 2000 reagent.

Isolation of Nuclear polyQ Aggregates and Identification of Aggregate-interacting Proteins by Mass Spectrometry—Nuclear polyQ aggregates were purified from HD 150Q-NLS cells as a final insoluble fraction from sequential extraction of nuclear proteins (15). The final nuclear insoluble fractions of HD150Q-NLS-D and HD150Q-NLS-D/I cells were boiled in the sample buffer for 5 min and subjected to SDS-PAGE using 10% polyacrylamide gel. The gels were stained with SYPRO Ruby protein gel stain (Molecular Probes), and bands in the gels were detected on a transilluminator. Each visible band of the insoluble fraction of HD150Q-NLS-D/I cells was excised. In the case of the insoluble fraction of HD150Q-NLS-D cells, gel regions corresponding to the molecular weight of the visible bands of the HD 150Q-NLS-D/I insoluble fraction were also excised. The in-gel digestion and subsequent mass spectrometry analysis were carried out as described previously (15). Mass spectrometry data were analyzed to predict the candidate sequence for the AIPs using MASCOT software (Matrix Science) and a public domain protein data base (National Center for Biotechnology Information) (20).

Preparation of Nuclear Soluble Fractions—To prepare the nuclear soluble fractions, we used, with minor modifications, a previously reported method that was developed for the preparation of nuclear extract and that was shown to be useful for *in vitro* transcription (21). Pelleted 1.2×10^8 HD 150Q-NLS-D and HD 150Q-NLS-D/I cells were suspended in 5 ml of 10 mM HEPES-KOH (pH 7.9), 1.5 mM $MgCl_2$, 10 mM KCl, and 0.5 mM dithiothreitol and incubated on ice for 10 min. The cells were collected by centrifugation for 10 min at 2,000 rpm, resuspended in 2 ml of same buffer, and lysed by 10 strokes with a glass Dounce homogenizer. The homogenates were centri-

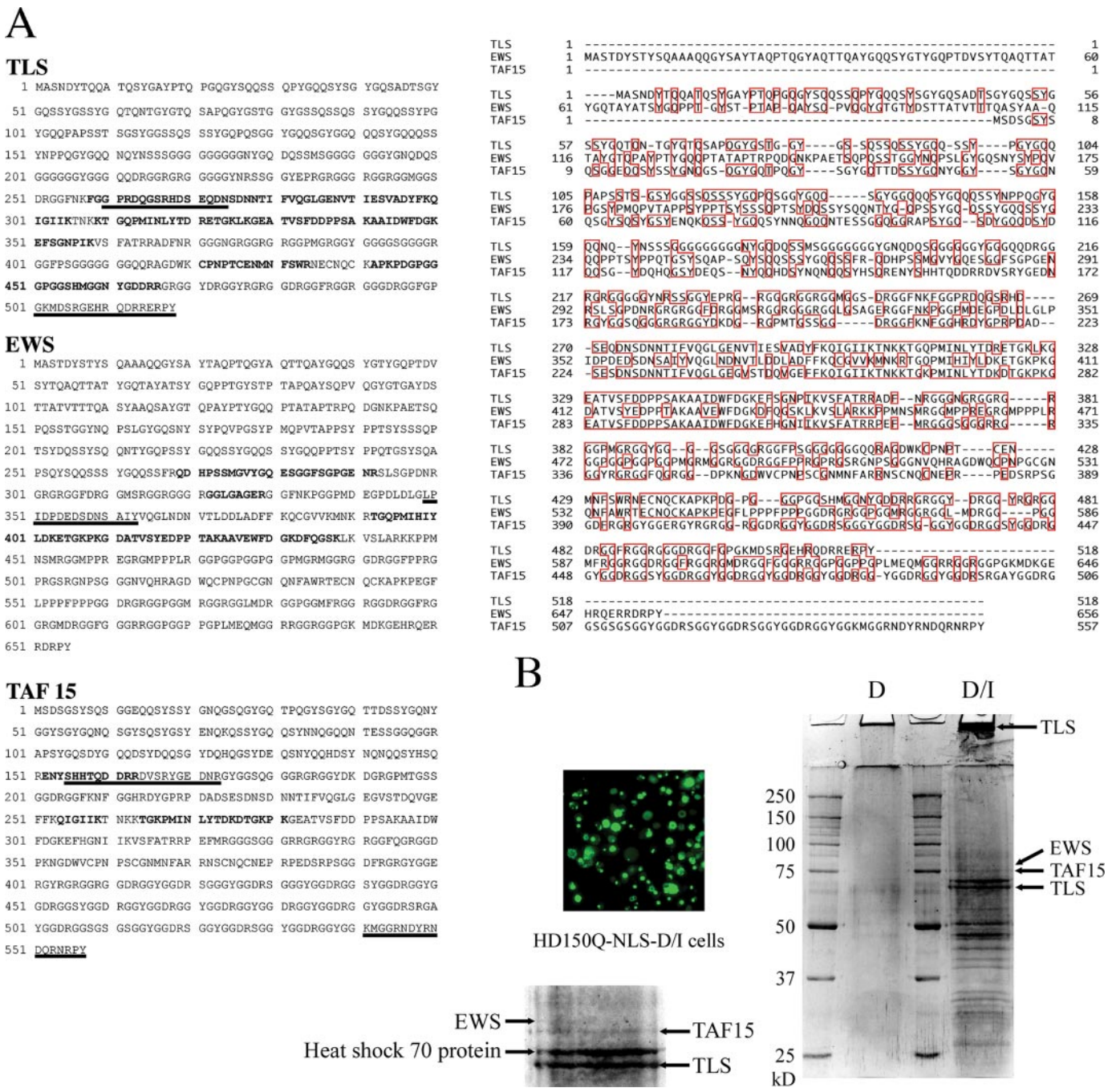

FIGURE 1. **TET family proteins were identified in purified nuclear polyQ aggregates.** *A*, the amino acid sequences and sequence alignment of TLS, EWS, and TAF15. The peptide sequences identified by mass spectrometry are indicated by *bold letters*, and peptide sequences used as antigens for generating antibodies are *underlined* (*left*). Identical amino acid sequences among these three proteins are *boxed* with *red* (*right*). The percentages of identical amino acid sequences as calculated by Genetyx software were as follows: TLS *versus* EWS, 44.4%; EWS *versus* TAF15, 40.1%; TAF15 *versus* TLS, 51.1%. *B*, microscopic image of HD150Q-NLS cells 3 days after differentiation and induction (HD150Q-NLS-D/I cells). In this condition, 39.13% (S.D. = 3.23%) of HD150Q-NLS-D/I cells have nuclear aggregates ($n = 12$). SDS-PAGE of a nuclear insoluble fraction containing 5×10^6 nuclear aggregates of HD150Q-NLS-D/I (differentiated and induced) cells (*right lane*), and a nuclear insoluble fraction of HD150Q-NLS-D (differentiated) cells (*left lane*) from the same amount of nuclei as used for the HD150Q-NLS-D/I nuclear insoluble fraction. TLS, EWS, and TAF15 are identified from the indicated bands of SDS-PAGE. The part of gel in which TLS, EWS, and TAF15 are identified is magnified. Parts of gel indicated by *arrows* were excised and then subjected to tandem mass spectrometry analysis.

fuged for 10 min at 2,000 rpm to pellet the nuclei. After the supernatants were removed, the pellets were subjected to a second centrifugation for 20 min at 25,000 × *g* to remove residual cytoplasmic material, and the resulting pellets were designated as crude nuclei. These crude nuclei were resuspended in 500 μl of 20 mM HEPES-KOH (pH 7.9), 25% glycerol, 0.42 M NaCl, 1.5 mM $MgCl_2$, 0.5 mM dithiothreitol, and 0.5 mM phenylmethylsulfonyl fluoride supplemented with Complete protease inhibitor mixture (Roche Applied Sciences) and homogenized by 10 strokes with a glass Dounce homogenizer. The suspension was incubated for 30 min at 4 °C with a vortex and centrifuged for 20 min at 25,000 × *g*. The resulting supernatants were dialyzed overnight against a 300 times volume of 20 mM HEPES-KOH (pH 7.9), 20% glycerol, 0.1 M KCl, 0.5 mM dithiothreitol, and

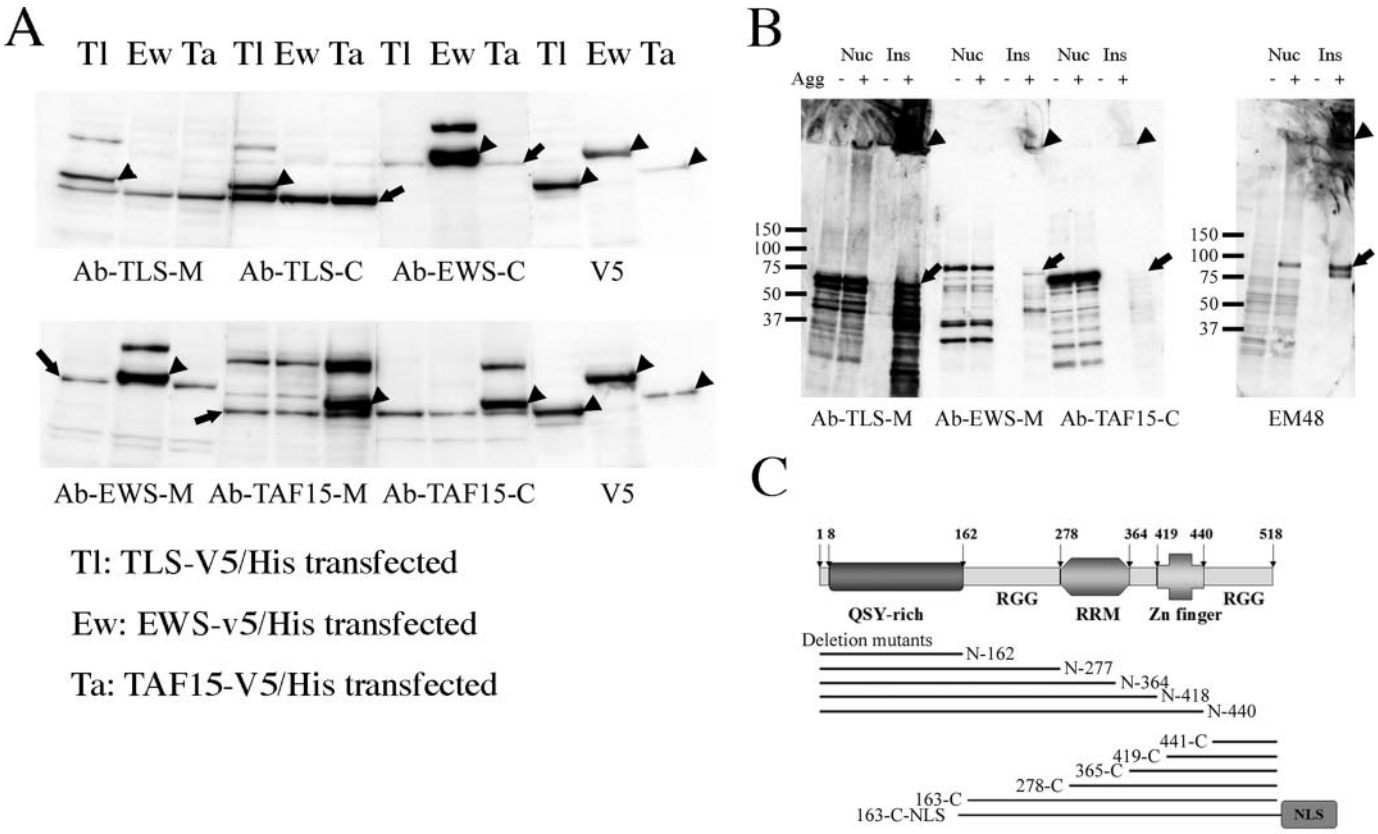
A
Tl Ew Ta Tl Ew Ta Tl Ew Ta Tl Ew Ta
Ab-TLS-M
Ab-TLS-C
Ab-EWS-C
V5
Ab-EWS-M
Ab-TAF15-M
Ab-TAF15-C
V5
Tl: TLS-V5/His transfected
Ew: EWS-v5/His transfected
Ta: TAF15-V5/His transfected
B
Nuc Ins Nuc Ins Nuc Ins Nuc Ins
Agg - + - + - + - + - + - +
150
100
75
50
37
Ab-TLS-M
Ab-EWS-M
Ab-TAF15-C
EM48
C
1 8
162
278
364 419 440
518
QSY-rich
RGG
RRM
Zn finger
RGG
Deletion mutants
N-162
N-277
N-364
N-418
N-440
441-C
419-C
365-C
278-C
163-C
163-C-NLS
NLS
D
TET family proteins (full length)
TLS deletion mutants
TLS
EWS
TAF15
EGFP
anti-V5
Merge
TLS (full length)
TLS (N-162)
TLS (163-C)
TLS (163-C-NLS)
(%)
100
80
60
40
20
0
EWS
TAF15
TLS
TLS N-162
TLS C-163-NLS
co-localization ratio n=3

0.5 mM phenylmethylsulfonyl fluoride supplemented with Complete protease inhibitor mixture. The dialysates were used as nuclear soluble fractions.

Western Blot Analysis—Cell lysates, nuclear fractions, nuclear soluble fractions, and purified aggregates were prepared as described above. These materials (20 μg/lane each fraction or 1×10^6 nuclear aggregate particles/lane) were subjected to SDS-PAGE and then electrophoretically transferred to a polyvinylidene difluoride (PVDF) membrane. The antibody dilutions were 1:2000 for anti-GFP, anti-v5-HRP, and HRP-conjugated secondary antibodies and 1:500 for anti-Hsp70, anti-TBP, anti-LaminB, and EM48 in 0.05% Tween 20/Tris-buffered saline (TBST). Immunoreactive proteins were detected with enhanced chemiluminescence reagents (Amersham Biosciences).

Human Brain—Human brain tissue was obtained from the Brain Collection at the University of Tsukuba. The full consent of the family was obtained at the time of autopsy, and the Hospital Human Subjects Ethics Committee approved the study. The HD case studied in this paper was examined by a neuropathologist to confirm HD pathology and assign a pathological grade (22).

Immunocytochemistry and Immunohistochemistry—Neuro2a cells growing on four-well chamber slides were co-transfected with 0.25 μg of TOPO-pcDNA3.1/v5-His vector containing TLS, TLS deletion mutants, EWS or TAF15, and tNhtt-153Q-EGFP-NLS. One day after transfection, the cells were washed twice with cold PBS, fixed for 20 min in 4% paraformaldehyde/PBS, washed twice with PBS, and permeabilized for 5 min with 0.5% Triton X-100/PBS. The frozen brains of R6/2 mice mounted in Tissue-Tek were cut into 10-μm sections with a freezing microtome. Paraffin-embedded human brain tissue sections from HD patient were deparaffinized and autoclaved in PBS for 5 min to enhance the staining. The immunostaining procedures were as described in our previous study (8, 15, 23). The antibody dilutions were 1:1000 for anti-v5 and monoclonal anti-ubiquitin (for brain tissue, anti-ubiquitin antibody dilution was 1:20000.) and 1:500 for monoclonal EM48 antibody and Alexa-488 or Alexa-546 conjugated secondary antibody in TBST. In some cases, staining was carried out using a Vectastain ABC kit (Vector laboratories, Burlingame, CA).

Aggregate Counting—HD150Q-NLS growing on 12-well plates were transfected with plasmids or siRNAs in the amounts indicated in the figures, treated with 5 mM dbcAMP and 1 μM ponasterone A for 3 days, washed twice with PBS, and fixed with 4% paraformaldehyde/PBS. Plasmid-transfected cells were immunostained with anti-v5 followed by nuclear staining with 10 μg/ml Hoechst 33342, trihydrochloride, and trihydrate (Molecular Probes) in PBS, and siRNA-transfected cells were stained with 10 μg/ml Hoechst 33342, trihydrochloride, and trihydrate in PBS. The quantification of the aggregation was performed by high content screening using an ArrayScan®V^{TI} high content screening reader (Cellomics Inc., Pittsburgh, PA). The ArrayScan®V^{TI} is able to measure the fluorescence intensity within each single cell in the visual field. A Target Activation Cellomics BioApplication V2 protocol was used, and the data were analyzed by Cellomics vHCS^{TM}:View software.

Protein Purification and in Vitro Binding Study—*Escherichia coli* BL21 (RP) carrying pGEX-6P-2 expression plasmids of tNhtt-18Q, 42Q, or 62Q was grown to an A_{600} of 0.5 at 37 °C and then induced with isopropyl β-D-thiogalactopyranoside (0.1 mM) for 2 days at 15 °C. Cultures of induced bacteria were centrifuged at 2,300 $\times$ *g* for 30 min, and the resulting pellets were resuspended in a three-times volume of buffer A (50 mM Tris-HCl, pH 7.5, 400 mM NaCl, 20% glycerol) containing 0.1% Tween 20, 10 mM $MgCl_2$, 1 mM phenylmethylsulfonyl fluoride, 0.5 mg/ml lysozyme, 20 ng/ml DNase I and protease inhibitor mixture, and stored at −80 °C. Bacterial lysates were thawed at 4 °C and centrifuged at 43,000 $\times$ *g* for 60 min. The supernatants were adjusted to pH 7.5 and applied to a column containing 25 ml of Glutathione-Sepharose High Performance (Amersham Biosciences), and the column was extensively washed with buffer A. The bound GST fusion protein was eluted with buffer A containing 10 mM glutathione. As for His-tagged TLS (His-TLS), *E. coli* BL21 (RP) carrying pET-15b expression plasmids of TLS and TLS deletion mutant were grown to an A_{600} of 0.8 at 37 °C and then induced with isopropyl β-D-thiogalactopyranoside (1 mM) for 24 h at 20 °C. Cultures of induced bacteria were collected, resuspended, and divided into a supernatant and pellet using the same procedures as for GST-tNhtt proteins. The pellets were resuspended in buffer A containing 3% Triton X-100, stirred at room temperature for 30 min, and centrifuged at 25,000 $\times$ *g* for 20 min. This step was repeated three times, and the pellets were washed with MilliQ water and centrifuged. The resulting pellets were resuspended in 6 M guanidine and centrifuged at 25,000 $\times$ *g* for 20 min. The supernatants were adjusted to pH 7.5 and applied to an nickel column, and then the nickel column was extensively washed with buffer A. The bound His-tagged protein was eluted with buffer A containing 0.2 M imidazole. The purified proteins were stocked at −80 °C.

FIGURE 2. **TET family proteins were associated with nuclear polyQ aggregates.** *A*, characterization of Ab-TLS-M, Ab-TLS-C, Ab-EWS-M, Ab-EWS-C, Ab-TAF15-M, and Ab-TAF15-C antibodies. Each antibody recognizes each endogenous and overexpressed protein. Ab-TLS-C slightly cross-reacts with EWS. *Tl*, *Ew*, and *Ta* indicate whole cell lysates of HD 150Q-NLS cells transfected with TLS-v5/His, EWS-v5/His, and TAF15-v5/His expressing plasmid, respectively. *Arrows* and *arrowheads* indicate each endogenous and overexpressed proteins, respectively. *B*, TLS, EWS, and TAF15 co-exist in purified nuclear polyQ aggregates. Western blot analysis was used to detect TLS, EWS, TAF15, and tNhtt-150Q-EGFP-NLS in the nuclei and in the insoluble fraction of HD150Q-NLS-D (Agg−) or HD150Q-NLS-D/I (Agg+) cells. *Arrowheads* indicate the gel-excluded materials immunoreactive with each antibody. *Arrows* indicate each antigenic protein. *Nuc*, nuclear fraction; *Ins*, insoluble fraction of the nuclei. *C*, schematic domain structure of TLS and TLS deletion mutants. *QSY-rich*, Gln, Ser, and Thy -rich domain; *RGG*, Arg-Gly-Gly repeats; *RRM*, RNA recognition motif; *Zn finger*, zinc finger domain. *D*, immunocytochemistry of Neuro2a cells co-transfected with expression plasmids of full-length TET family proteins (TLS-v5/His, EWS-v5/His, and TAF15-v5/His; *left panel*) or TLS deletion mutants (TLS-V5/His (TLS full-length), TLS-N-162-V5/His (TLS-N-162), TLS-163-C-V5/His (TLS-C-163), and TLS-163-C-NLS-V5/His (TLS-163-C-NLS); *right panel*), and pcDNA3.1-tNhtt-150Q-EGFP-NLS. Overexpressed TET family proteins and TLS deletion mutants are labeled by anti-v5 antibody (Alexa fluor 546 as the secondary antibody). In the *right panel*, the nuclei are stained with 4′,6-diamidino-2-phenylindole. The *bars* equal 10 μm. The co-localization ratio was taken as the number of the cells having v5-immunoreactive aggregates/the number of the transfected cells having aggregates and is shown in the graph.

100 μl of 50% v/v Glutathione-Sepharose 4B (Amersham Biosciences) was incubated with 200 μl of 50 μg/ml GST-tNhtt-18Q, 42Q, or 62Q in buffer B (50 mM Tris-HCl, pH 7.0, 150 mM NaCl, 20% glycerol) at 4 °C for 60 min with rotation and then placed in a spin column, centrifuged, and washed twice with 200 μl of buffer B. Each resin in the spin column was mixed with 200 μl of 50 μg/ml His-TLS in buffer B, incubated at 4 °C for 2 h with rotation, centrifuged, washed twice with 200 μl of buffer B, and eluted three times with 200 μl of buffer B containing 10 mM glutathione. Each through-fraction was collected and analyzed. A complementary experiment was carried out for the confirmation. 100 μl of 50% v/v, BD TALON (BD Biosciences, San Jose, CA) was used to bind to His-TLS, and the binding assay was performed using the procedure described above.

Far Western Blot Analysis and Filter Trap Assay—200 μl of 50 μg/ml GST-tNhtt-18Q, 42Q, or 62Q in buffer B was incubated with or without 2 units of PreScission protease (Amersham Biosciences Bioscience) at 4 °C for 2 h. Where indicated, another incubation at 30 °C for 16 h was added. The reactions were terminated by adding an equal volume of SDS sample buffers into each sample. Each sample was boiled for 5 min and then subjected to SDS-PAGE followed by the transfer to a PVDF membrane. For the filter trap assay, 200 μl of the indicated concentrations of GST-tNhtt fusion proteins were incubated with 2 units of PreScission protease at 30 °C for 16 h. Each sample was filtered by a cellulose acetate membrane. After the PVDF membranes or cellulose acetate membranes were blocked with TBST containing 2% nonfat milk, the membranes were probed with the indicated antibodies or incubated overnight at 4 °C with 0.01 μM His-TLS in TBST. The membranes incubated with His-TLS solutions were washed extensively with TBST and probed with Ab-TLS-C. 1C2 was diluted 1:2000 in TBST, and the dilutions of the other antibodies were the same as used in the Western blot analysis.

Thioflavin T Assay—The thioflavin T assay was carried out essentially as described previously (24). Stocked GST-tNhtt-42Q and His-TLS were diluted and adjusted with buffer B and then filtered through a PVDF membrane with 22 μm pores before the assay. Each protein solution was mixed with 20 μl of 250 μM thioflavin T (Sigma-Aldrich) in 250 mM glycine (pH 8.0), and buffer B was added for a total volume of 200 μl. Where indicated, 10 μl of 0.2 unit/μl PreScission protease in buffer B and/or sonicated tNhtt fibrils was included in the solutions. Fluorescence was monitored using a 96-well fluorescence plate reader Spectra Max M2 (Molecular Device, Sunnyvale, CA; 442-nm excitation and 485-nm emission). 96-well plates were tightly covered with polyolefin sealing tape (Nalge Nunc International, Naperville, IL) to prevent evaporation of solutions. Thioflavin T assays were carried out at 30 °C and read automatically every 2 min with 5 s of shaking between measurements.

Electron Microscopy—The negative staining for the tNhtt-42Q fibrils and TLS was performed as reported previously (25), and the images were recorded on a LEO 912AB electron microscope (LEO, Cambridge, UK). Each of the indicated reactants was spun down by centrifugation at 186,000 × *g* for 30 min, and resuspended in PBS. The samples on copper grids were treated with EM48, 1C2, or Ab-TLS-M antibodies, followed by 5- or 10-nm gold-conjugated secondary antibodies.

RESULTS

Identification of TET Family Proteins in Purified tNhtt-150Q-EGFP-NLS Aggregates by Mass Spectrometry—Nuclear polyQ aggregates were isolated from the nuclei of the HD150Q-NLS cells by sequential extractions of soluble nuclear proteins as described in our previous study (15). Following SDS-PAGE of the purified nuclear polyQ aggregates from HD-150Q-NLS-D/I (Fig. 1*B*, differentiated and induced to express polyQ proteins) cells, each band was excised as indicated in Fig. 1*B* (*left panel*, *arrows*), and the proteins in gel pieces were digested with trypsin and subjected to tandem mass spectrometry analysis. As a result, we identified TLS as the major component of the major band and the gel-excluded materials (Fig. 1). We suspected that TLS was one of the major nuclear polyQ aggregate-interacting proteins. EWS and TAF15, which have high similarity to TLS (Fig. 1*A*, *right panel*) and which are known as TET family proteins (along with TLS), were also found in purified nuclear polyQ aggregates (Fig. 1). But EWS and TAF15 were not found as the major component of each band. The major component of each band was heat shock 70 protein (Hsc70) in both cases. TET family proteins were not found in the insoluble fraction of HD150Q-NLS-D (differentiated, but not induced) cells.

TET Family Proteins Were Bound to polyQ Aggregates in neuro2a Cells through a QSY-rich Domain—We performed Western blot analysis to verify the presence of these proteins in the aggregates. To this end, we generated polyclonal antibodies Ab-TLS-M and Ab-TLS-C against TLS, Ab-EWS-M against EWS, and Ab-TAF15-M and Ab-TAF15-C against TAF15 (Fig. 2*A*). We also used a commercially available goat polyclonal anti-EWS antibody (Ab-EWS-C). Western blot analysis confirmed that TLS, EWS, and TAF15 were co-purified with nuclear polyQ aggregates (Fig. 2*B*). These findings suggested that TLS, EWS, and TAF15 were capable of binding to the polyQ aggregates and shifted to the SDS-insoluble fraction upon formation of polyQ aggregates. Consistent with the mass spectrometry results, in the TET family proteins, TLS was present at the highest level in the purified aggregates fraction. To check whether TET family proteins co-localize with polyQ aggregates, we generated expression plasmids of TET family proteins. An immunocytochemical study revealed that the overexpressed full-length TLS-v5/His, EWS-v5/His, and TAF15-v5/His co-localized with nuclear polyQ aggregates (Fig. 2*D*, *left panel*). Next, to determine the aggregate-interacting domain of TET family proteins, we generated expression plasmids of TLS deletion mutants as indicated in Fig. 2*C*. TLS deletion mutants that contained the N-terminal QSY-rich domain of TLS (TLS-N-162-v5/His∼TLS-N-440-v5/his) co-localized with polyQ aggregates of HD150Q-NLS cells (Fig. 2*D*; TLS (N-162) and data not shown). Because, in agreement with a previous report (26), TLS deletion mutants without a QSY-rich domain (TLS-163-C-v5/His∼TLS-441-C-v5/his) were distributed in the cytoplasm (Fig. 2*D*, *right panel*, and data not shown), we generated TLS-163-C-NLS-v5/His (TLS-C-163-NLS) to examine whether a TLS deletion mutant without a QSY-rich domain could bind to nuclear polyQ aggregates. The results

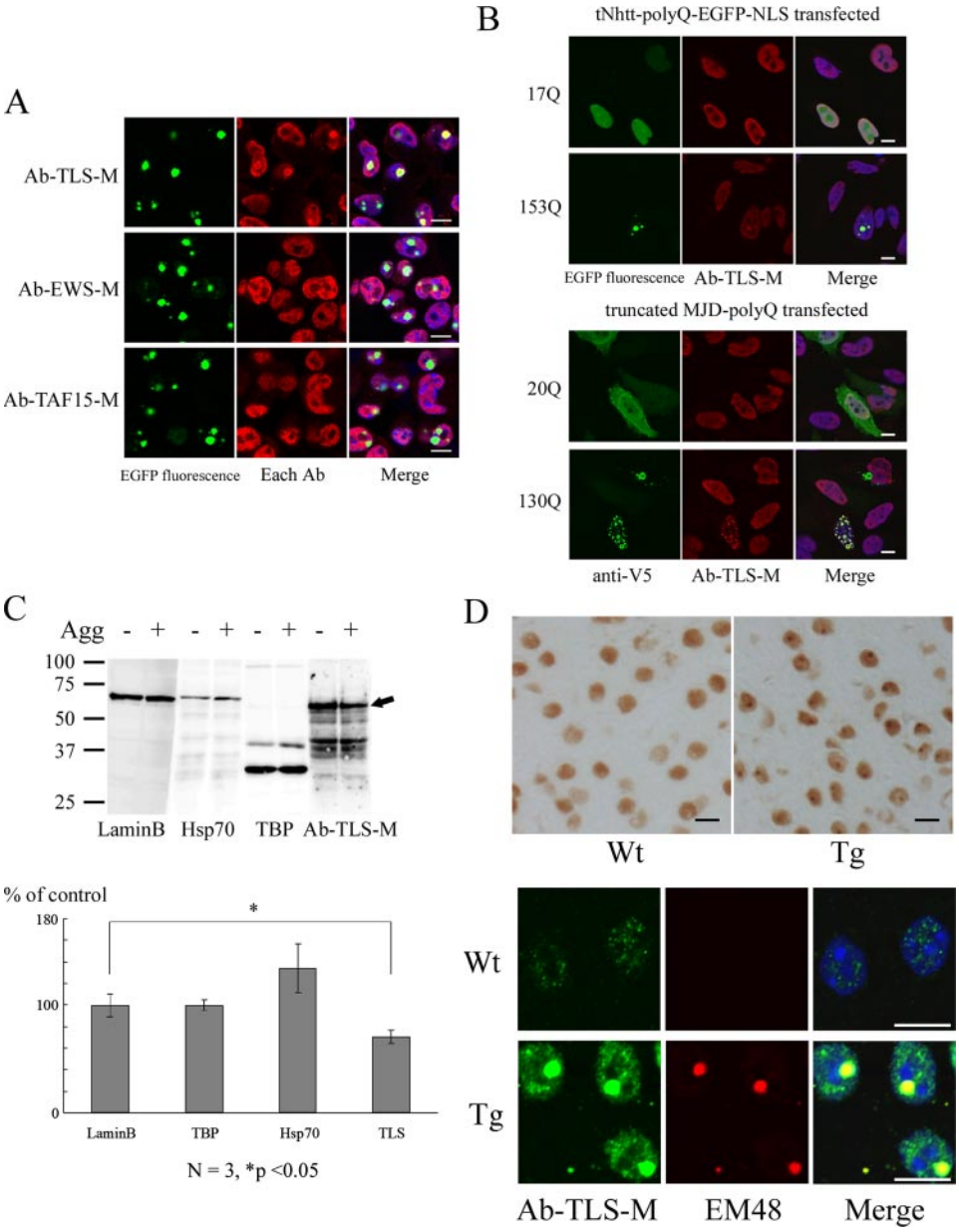

FIGURE 3. **Endogenous TLS co-localized with poly Q aggregates formed by tNhtt and truncated ataxin-3 and TLS was associated with neuronal intranuclear inclusions of R6/2 mice.** *A*, immunocytochemistry of HD150Q-NLS cells expressing tNhtt-150Q-EGFP-NLS. Endogenous TET family members were labeled by the indicated antibodies (Alexa fluor-546). Endogenous TLS (but not EWS and TAF15) co-localized with nuclear polyQ aggregates of HD 150Q-NLS cells. The *scale bars* equal 10 μm. *B*, immunocytochemistry of HeLa cells transfected with pcDNA3.1-tNhtt-17Q-EGFP-NLS, pcDNA3.1-tNhtt-153Q-EGFP-NLS, pcDNA3.1-truncated ataxin3–20Q-v5, or pcDNA3.1-truncated ataxin3–130Q-v5. Endogenous TLS was labeled by Ab-TLS-M (Alexa fluor-546). Truncated ataxin3 proteins were labeled by anti-v5 antibody (Alexa fluor 488). Endogenous TLS co-localized with nuclear polyQ aggregates that were formed by truncated ataxin-3 proteins with 130Q. The *scale bars* equal 10 μm. *C*, Western blot analysis of nuclear soluble fractions from HD150Q-NLS-D cells (*Agg*−) and HD150Q-NLS-D/I cells (*Agg*+). The *arrow* indicates TLS labeled with Ab-TLS-M (*upper panel*). The results of densitometric analysis of each immunoreactive band are shown in the graph (*Agg*+/*Agg*−; *lower panel*). *D*, immunohistochemistry of frozen brain sections prepared from R6/2 transgenic mice and their age-matched controls at 8 weeks (*upper panel*), or 15 weeks of age (*lower panel*). The sections were labeled with Ab-TLS-M followed by detection with ABC kit (*upper panel*) or double labeled with EM48 (Alexa fluor-546) and Ab-TLS-M (Alexa fluor-488) followed by 4′,6-diamidino-2-phenylindole staining, and the results indicated that TLS is associated with neuronal intranuclear inclusions. The *scale bars* equal 10 μm.

showed that the TLS deletion mutant without a QSY-rich domain did not bind to nuclear polyQ aggregates even when it was distributed to the nuclei (Fig. 2*D*, *right panel* and *graph*). We concluded that the polyQ aggregate-interacting domain of TLS was a QSY-rich domain.

Endogenous TLS Associated with tNhtt and Ataxin 3 Aggregates and Soluble TLS Were Decreased in the HD Cell Model—Next we checked whether endogenous TET family proteins were co-localized to nuclear polyQ aggregates. The endogenous TLS was clearly accumulated in nuclear polyQ aggregates (Fig. 3*A*). As for EWS and TAF15, although they existed around nuclear polyQ aggregates, clear accumulation was not observed (Fig. 3*A*). The binding of endogenous EWS and TAF15 to nuclear polyQ aggregates was not as strong as that seen in TLS, and we could not detect a clear co-localization by immunocytochemistry. We also found that TLS co-localized with polyQ aggregates formed by truncated ataxin 3 proteins with expanded polyQ tract in HeLa cells (Fig. 3*B*). Because the polyQ tract is the only common sequence between tNhtt and truncated ataxin 3 proteins, we considered that TLS probably interacted with polyQ tracts at some stage of polyQ aggregate formation. We also checked whether the amount of TLS in nuclear soluble fraction changed. For this purpose, we prepared a nuclear soluble fraction from HD150Q-NLS-D and HD150Q-NLS-D/I cells. In contrast to TBP, TLS was significantly decreased in HD150Q-NLS-D/I cells comparing to Lamin B (Fig. 3*C*).

TLS Was Co-localized with NIIs in the HD Transgenic Mice—Next we examined whether TLS was associated with polyQ aggregates in HD exon 1 transgenic mice (R6/2 mice) (27). Immunostaining of R6/2 brain sections showed that only transgenic mouse had Ab-TLS-M immunoreactive NIIs (Fig. 3*D*, *upper panel*). We also confirmed that TLS co-localized with EM48 immunoreactive NIIs (Fig. 3*D*, *lower panel*). Similar to the results of immunocytochemistry in the cellular experiment above, EWS and TAF15 did not show clear co-localization with NIIs (data not shown).

TLS Bound to tNhtt-42Q and 62Q Aggregates in Vitro—To determine that TLS could directly bind to polyQ proteins, we carried out an *in vitro* binding study. Fig. 4*A* shows the results of

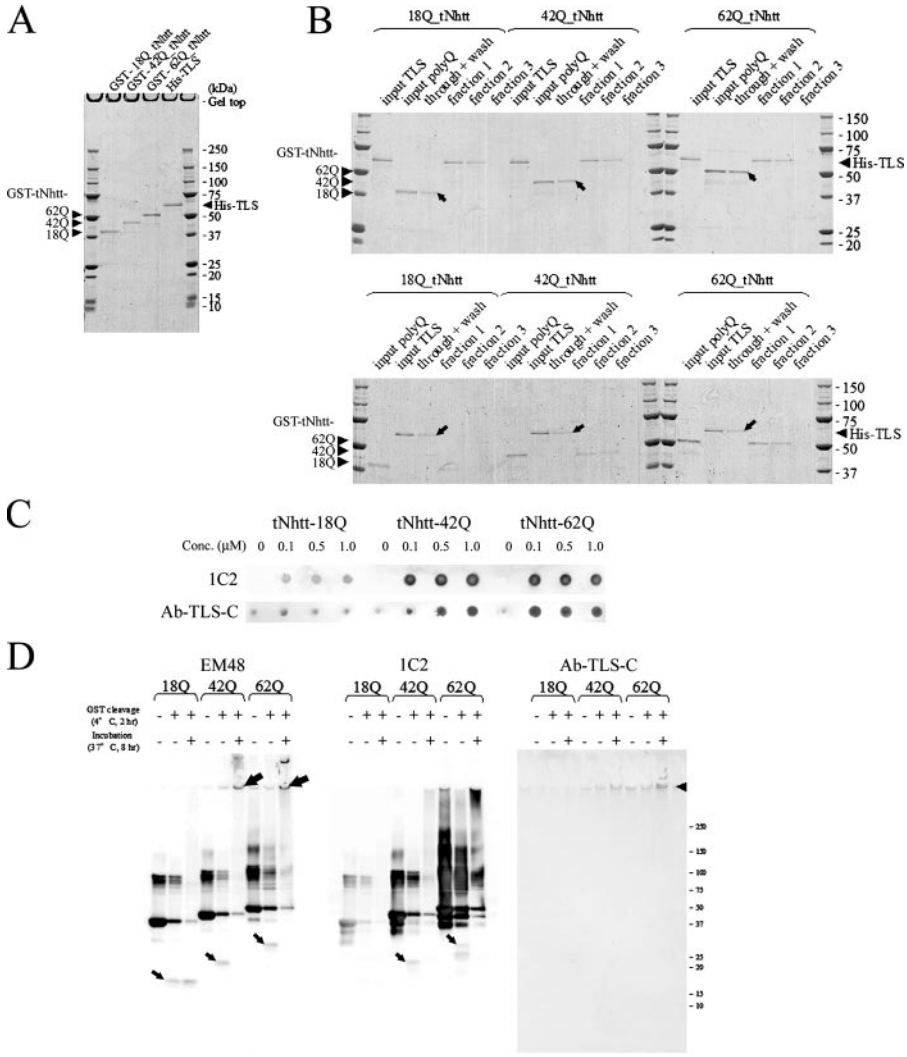

FIGURE 4. **TLS bound to aggregated polyQ proteins *in vitro*.** *A*, SDS-PAGE of GST-tagged tNhtt-18Q, 42Q, 62Q and His-tagged TLS (*arrowheads*). The gel was stained with Coomassie Brilliant Blue R250 (Nacalai Tesque). *B*, *in vitro* binding study of His-TLS and GST-tNhtt-18Q, 42Q, or 62Q proteins. GST-tNhtt proteins could be detected only in washing fractions (*arrows*) and were not eluted with His-TLS (*upper panel*). In the complementary experiment, His-TLS could be detected only in washing fractions (*arrows*) and were not eluted with any length of GST-tNhtt proteins (*lower panel*). *C*, filter trap assay of aggregated polyQ proteins. GST-tNhtt-18Q, 42Q, and 62Q proteins were incubated with PreScission protease at 30 °C for 16 h at the indicated concentrations. Aggregated proteins were trapped on a cellulose acetate membrane. The membranes were labeled by 1C2 antibody (*upper panel*) or incubated with 10 μM TLS solution and labeled by Ab-TLS-C (*lower panel*). *D*, Western blot and Far Western analysis of GST-tNhtt proteins. GST-tNhtt proteins that underwent the indicated treatments were subjected to SDS-PAGE and transferred to PVDF membranes. The membranes were labeled by EM48 (*right*) or 1C2 (middle) antibody. One of the membranes was labeled by Ab-TLS-C after incubation with 10 mM His-TLS solution. The *smaller arrows* indicate tNhtt fragments resulting from GST digestion. The *larger arrows* indicate tNhtt-42Q and tNhtt-62Q aggregates detected as gel-excluded materials. TLS bound to the aggregates of tNhtt-42Q and tNhtt-62Q (*arrowhead*).

the SDS-PAGE of purified GST-fused truncated huntingtin exon 1 with 18Q, 42Q, and 62Q (GST-tNhtt-18Q, 42Q, and 62Q) and His-tagged TLS (His-TLS). GST could be removed by PreScission protease digestion. Using these proteins, we examined whether His-TLS could bind to GST-tNhtt proteins (Fig. 4*B*). When His-TLS-bound resin was incubated with GST-tNhtt, none of the GST-tNhtt proteins were eluted with His-TLS (Fig. 4*B*, *upper panel*). As a complementary experiment, each GST-tNhtt protein-bound resin was incubated with His-TLS. His-TLS was not eluted with each GST-tNhtt protein. These results indicated that the monomer GST-tNhtt could not bind to TLS even if it had an expanded polyQ tract.

To confirm that TLS directly bound to polyQ aggregates, we carried out a filter trap assay and far Western analysis. It has been shown that GST-tNhtt proteins with an expanded polyQ tract start to form amyloid fibrils after removal of their GST (2, 28). In the present study, after GST-tNhtt-18Q, 42Q, and 62Q proteins were incubated with PreScission protease at 30 °C for 16 h to remove GST and to initiate aggregate formation, aggregated proteins were trapped on a cellulose acetate membrane. The membranes were labeled with 1C2 antibody (Fig. 4*C*, *upper panel*) or incubated with 10 μM TLS solution and labeled with Ab-TLS-C (Fig. 4*C*, *lower panel*). TLS could directly bind to polyQ proteins trapped on the cellulose acetate membrane. Far Western analysis also showed that His-TLS could directly bind to aggregated tNhtt proteins (Fig. 4*D*, *arrowheads*) but not to monomer GST-tNhtt or tNhtt fragments, indicating that tNhtt proteins acquired the ability to bind to TLS after forming insoluble aggregates or amyloid fibrils.

TLS Inhibited the tNhtt-42Q Amyloid Formation in Vitro Being Sequestrated to tNhtt-42Q Amyloids—To determine the effect of TLS on polyQ amyloid formation *in vitro*, we used a thioflavin T assay to monitor the kinetics of *in vitro* amyloid formation of tNhtt-42Q, such as previously reported for the monitoring of prion amyloid formation (24, 29). When His-TLS was added, His-TLS dose-dependently inhibited the amyloid formation of tNhtt-42Q (Fig. 5*A*, *upper graph*). To omit the possibility that addition of His-TLS nonspecifically affected the tNhtt 42Q amyloid formation, we used myoglobin as a negative control. TLS decreased the velocity of amyloid growth, whereas myoglobin did not affect it (Fig. 5, *A*, *lower graph*, and *B*). This result further suggests that TLS could directly bind to tNhtt-42Q at some stage of amyloid formation. Consistent with the *in vitro* study, the reduction of TLS by siRNA accelerated tNhtt-150Q-EGFP-NLS aggregate formation in HD150Q-NLS cells (Fig. 5*C*), indicating that endogenous TLS had inhibitory effects on polyQ amyloid formation in the cells. To determine which step of amyloid formation was mainly inhibited by TLS, we used tNhtt-42Q amyloid seeds to eliminate the lag phase for amyloid formation. If tNhtt-

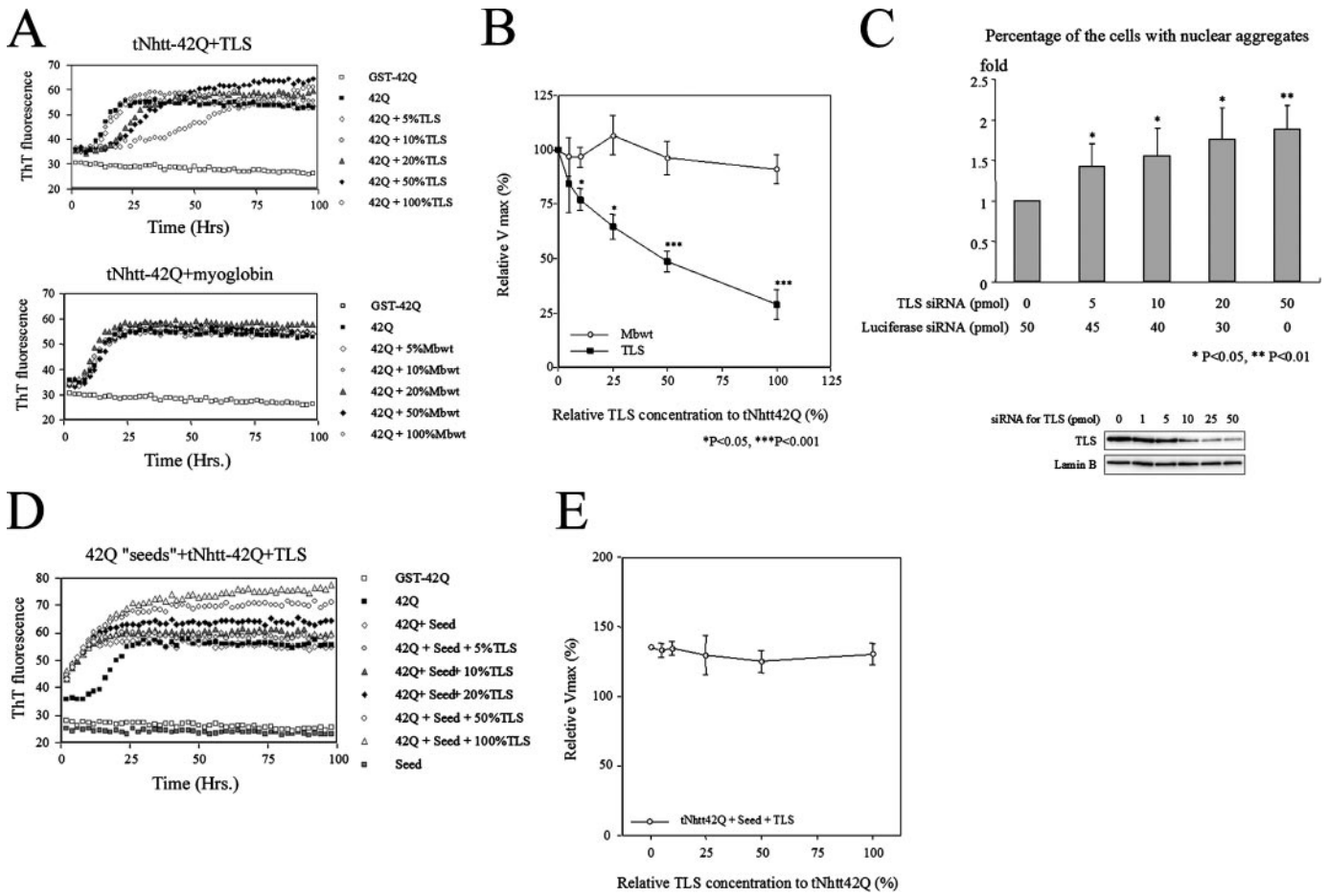

FIGURE 5. **TLS inhibited polyQ aggregate growth *in vitro* and *in vivo*.** *A*, effects of TLS and myoglobin on tNhtt-42Q amyloid formation were monitored by Thioflavin T fluorescence. Thioflavin T fluorescence was monitored every 2 min, but the fluorescence values are shown at intervals of 2 h. *B*, relative V_{max} of tNhtt-42Q amyloid formation calculated from a thioflavin T assay ($n = 3$). *C*, the effects of TLS-reduction by siRNA on polyQ aggregate formation in HD150Q-NLS cells. The number of the cells with nuclear aggregates (which equals the number of nuclear polyQ aggregates/the number of the nuclei) was calculated. The ratios relative to the control are shown ($n = 4$). To show the effect of siRNA for TLS, Western blot analysis of cell lysates from Neuro2a cells treated with siRNA for TLS is present. *D*, the effects of TLS and tNhtt-42Q seeds on tNhtt-42Q amyloid formation were monitored by Thioflavin T fluorescence. *E*, V_{max} of amyloid formation of tNhtt 42Q with seeds calculated from thioflavin T assay ($n = 3$).

42Q seeds were added to polyQ solutions, the lag phase for amyloid formation disappeared, as previously reported for prion amyloid formation (30) (Fig. 5*D*). Under this condition, TLS did not affect the amyloid growth (Fig. 5*E*), indicating that TLS bound to small aggregates and interfered with the early stage of amyloid formation (*i.e.* nuclear formation). As a consequence, TLS reduced the rate of the subsequent amyloid growth.

TLS Bound to Amorphous polyQ Aggregates before Formation of Amyloid Fibrils—The above findings were confirmed by immunoelectron microscopy. When 2 μM GST-tNhtt-42Q was incubated with PreScission protease at 30 °C for 24 h, tNhtt-42Q showed an amyloid fibril structure, and EM48 bound to tNhtt-42Q amyloid fibrils thoroughly (Fig. 6*A*), but 1C2 bound to the tips of amyloid fibrils (Fig. 6*B*), where β-sheet structures are thought to be exposed (25). When 2 μM GST-tNhtt-42Q was incubated with PreScission protease and 0.4 μM TLS at 30 °C for 24 h and then stained with Ab-TLS-C, Ab-TLS-C also bound to the tNhtt amyloid fibrils thoroughly (Fig. 6*C*), indicating that TLS was sequestered into tNhtt amyloid fibrils. Mature tNhtt-42Q amyloid fibrils were also incubated with 0.4 μM TLS at 30 °C for 3 h, and TLS was found to bind to tNhtt-42Q amyloid fibrils, although it preferentially bound to the tips or angles of tNhtt-42Q amyloid fibrils (Fig. 6*E*). These findings indicated that TLS bound to the polyQ aggregates at the points where the polyQ tracts were exposed. Our thioflavin T assay results indicated that TLS could bind to tNhtt-42Q aggregates before tNhtt-42Q formed amyloid fibrils. To confirm this, 2 μM GST-tNhtt-42Q was incubated with PreScission protease and 0.4 μM TLS at 30 °C for 5 h. tNhtt formed amorphous aggregates, before polyQ protein formed mature amyloid fibrils (25). Double immunostaining with EM48 and Ab-TLS-C revealed that TLS had already bound to these amorphous aggregates (Fig. 6*F*), consistent with the results of the thioflavin T assay.

TLS Immunoreactivity in HD Brain—Finally, we investigated whether TLS bound to NIIs of HD brain. HD brain sections of cerebral cortex were stained with anti-ubiquitin antibody to identify the lesion where ubiquitin immunoreactive NIIs existed (Fig. 7. *upper panel*). After we found the ubiquitin immunoreactive NIIs, we conducted immunostaining of HD brain using Ab-TLS-M. We confirmed that Ab-TLS-M immunoreactive NIIs existed in HD brain where ubiquitin immunoreactive NIIs were often observed (Fig. 7, *lower panel*).

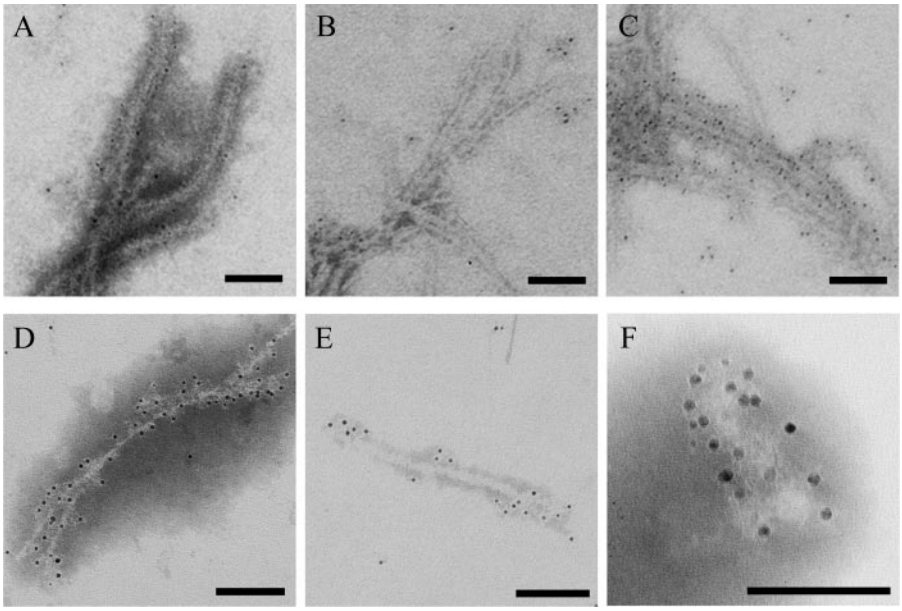

FIGURE 6. **TLS bound to polyQ amyloid and amorphous aggregates.** Immunoelectron microscopy of tNhtt-42Q amyloids and amorphous aggregates. *A* and *B*, 2 μM GST-tNhtt-42Q was incubated with PreScission protease at 30 °C for 24 h and was stained with EM48 (*A*) or 1C2 (*B*). EM48 bound to tNhtt amyloids thoroughly, but 1C2 bound to the tips of amyloid fibrils (*arrow*). *C*, 2 μM GST-tNhtt-42Q was incubated with PreScission protease and 0.4 μM TLS at 30 °C for 24 h and was stained with Ab-TLS-C. Ab-TLS-C also bound to tNhtt amyloid thoroughly. *D* and *E*, to make mature tNhtt amyloids, 2 μM GST-tNhtt-42Q was incubated with PreScission protease at 30 °C for 24 h. Mature tNhtt amyloids were incubated with 0.4 μM TLS at 30 °C for 3 h, and labeled with the EM48 (*D*) or Ab-TLS-C (*E*). *F*, immunoelectron microscopy of tNhtt aggregates double stained with EM48 and Ab-TLS-C. EM48 was detected by 10 nm of the gold-conjugated secondary antibody, and Ab-TLS-C was detected by 5 nm of the gold-conjugated secondary antibody. 2 μM GST-tNhtt-42Q was incubated with PreScission protease and 0.4 μM TLS at 30 °C for 5 h. All of the *scale bars* equal 100 nm.

DISCUSSION

In a previous study, we established a method for purifying nuclear polyQ aggregates from an HD cell model, and we showed that this method could identify not only a group of proteins that were already known to be AIPs, including members of the heat shock protein family, but also new AIPs, such as ubiquitin-interacting proteins, which confirmed the importance of direct analysis of purified aggregates (15). In this study, we demonstrated that TLS was one of the major AIPs in an HD cell model and that EWS and TAF15, proteins of the TLS family, were also present in AIPs. When overexpressed, these three proteins were co-localized with polyQ aggregates. An immunocytochemical study on a cellular and mouse model (R6/2) clearly showed co-localization of TLS with polyQ aggregates but failed to show co-localization of endogenous EWS and TAF15 with polyQ aggregates. These results indicated that although these TET family proteins have a certain homology among them, they differ in their ability to bind with polyQ aggregates, with TLS showing the highest rate of such binding.

It has been reported that normal cellular proteins that contain a homopolymeric stretch of glutamines such as ataxin 3, TBP, and CBP, bind to pathogenic polyQ proteins or polyQ aggregates, and recruitment of these proteins into polyQ aggregates depended on the interactions between polyQ tracts (31, 32). Although TLS does not have a homopolymeric stretch of glutamines, we demonstrated that a QSY-rich domain in TLS was necessary to bind to polyQ aggregates. We also revealed that the amount of TLS in the nuclear soluble fraction was decreased by the formation of polyQ aggregates, but the amount of TBP was not changed. The results indicated that although TLS contains no homopolymeric polyQ tracts, it could be more strongly sequestered to polyQ aggregates than TBP.

The interactions between AIPs and polyQ aggregates are of several different types, such as specific interactions with disease gene products such as huntingtin-associated protein 1 (33) and C-terminal binding protein (34), interactions between polyglutamine stretches such as CBP or TBP, and interactions between ubiquitin and ubiquitin-interacting proteins such as ubiquilins. In these previous studies, chaperones or ubiquitin-proteasome proteins were associated with polyglutamine aggregates, probably through their recognition of abnormally folded proteins.

We therefore investigated whether TLS could directly bind to the tNhtt protein *in vitro*. Although soluble GST-tNhtt-polyQ proteins did not interact with His-TLS, the filter trap assay and far Western blot analysis revealed a direct interaction between His-TLS and the tNhtt-42Q or tNhtt-62Q aggregates. In the previous report, it was revealed that removal of GST from the GST-tNhtt-polyQ protein triggered a β-sheet conversion and produced amyloid fibrils of tNhtt-polyQ proteins (28). Thus the conformational change of polyglutamine seems to be necessary for the interaction with TLS.

It has been revealed that there are several steps in the amyloid formation of expanded polyQ proteins (35). After some modification of expanded polyQ protein, for example, cleavage or phosphorylation, β-sheet conversion of the expanded polyQ protein occurs, and then the formation of mature amyloid fibrils occurs, probably via the structures of globular intermediates and protofibrils (35). Recent studies have suggested that the intermediate products of amyloids, including soluble β-sheet conformers (36) and globular intermediates (37), have a toxic effect on cells. We observed that tNhtt-42Q also formed an amorphous structure before forming mature amyloid fibrils and showed that TLS bound to the amorphous tNhtt-42Q aggregates (Fig. 6*F*). The electron microscopic observation revealed that TLS binds to preformed amyloid fibrils at their tips, although TLS was integrated into fibrils when incubated together with tNhtt-42Q, which was continuously supplied by cleavage from GST-tNhtt-42Q over a long period of time, suggesting that TLS interacts with some conformation of exposed polyglutamine.

The molecules that can interact with polyQ proteins, such as Congo red (38), QBP1 (36, 39), trehalose (6), Hsp70 and Hsp40

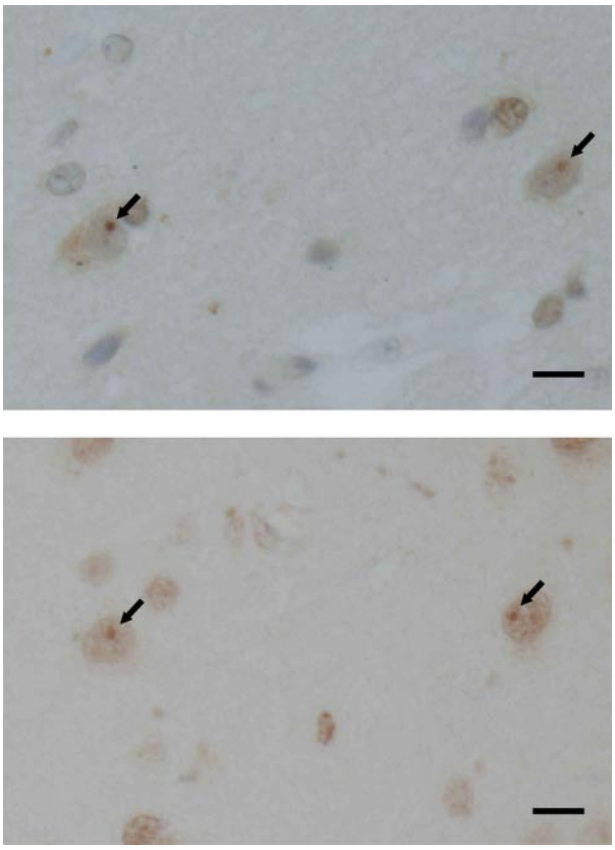

FIGURE 7. **TLS immunoreactivity in HD brain.** Sections from the cerebral cortex of HD case (57-year-old man with 54/26 CAG repeats) were stained with anti-ubiquitin antibody (*upper panel*) and Ab-TLS-M (*lower panel*). The *arrows* indicate NIIs. In the case of anti-ubiquitin antibody staining, the nuclei were counter-stained by hematoxylin. The *scale bars* equal 10 μm.

(28), are known to change the kinetics of polyQ amyloid formation *in vitro* and *in vivo*. Given the results of these studies, the polyQ protein starts to form aggregates or amyloid fibrils solely. But if some protein that has ability to bind to polyQ protein or polyQ aggregates exists, aggregation step could be inhibited because of the inhibition of polyQ-polyQ interaction, resulting in the inhibition of the growth of fibril formation and inclusion observed here. We showed that TLS decreased the velocity of amyloid growth *in vitro*. Using siRNA for TLS, we also revealed that endogenous TLS affected the tNhtt-150Q-NLS aggregate formation in HD150Q-NLS cells. This result strongly supported the idea that TLS interacts with polyQ protein *in vivo*. As a consequence of this interaction, the amyloid formation of polyQ proteins is delayed, and TLS is recruited to insoluble polyQ aggregates.

The TLS gene was originally identified as encoding the N terminus of TLS-CHOP, a fusion oncoprotein that is expressed as a consequence of the t (12, 16) translocation, which is invariably associated with human myxoid and round cell liposarcomas. It is known that TLS interacts with many proteins that participate in transcriptional machinery (40), RNA processing (41, 42), and RNA transport (26, 43). In primary neurons, TLS was located to the neuronal dendrites as an RNA-protein complex in response to metabotrophic glutamate receptor 5 activation (44), and primary neurons from TLS-deficient mice showed reduced spine number and abnormal spine morphology (45), indicating TLS has an important role in neurons. In our study we revealed that TLS bound strongly to polyQ aggregates, and soluble TLS was decreased in nuclei. It is possible that inadequate supply of TLS results in the dysfunction of transcription, RNA processing, or RNA transport, and these dysfunctions may cause instability of dendritic spines, which were seen in R6/2 mice (46) and HD patients (47). Although our data were obtained from htt exon1 expressing cell (HD150Q-NLS) and model mouse (R6/2), recent report suggests that transcriptional abnormality of this mouse recaptured the expression change observed in human HD brain (48). Considering that truncated htt exon1 product with expanded polyQ causes the alteration of gene expression, which is seen in HD, the result that TLS was decreased in the nuclei with polyQ aggregates could have a significant role in HD.

Finally, we revealed that TLS bound to NIIs of HD brain. This result suggests that TLS participates in the pathogenesis of polyQ diseases. Further study is necessary to clarify this loss-of-function effect *in vivo*.

Acknowledgments—We are indebted to Prof. A. Tamaoka for providing HD brain tissue. We are also indebted to the Research Resource Center of our institute for DNA sequencing analysis, peptide synthesis, generation of antibodies, and electron microscopic analysis.

REFERENCES

1. The Huntington's Disease Collaborative Research Group (1993) *Cell* **72,** 971–983
2. Scherzinger, E., Lurz, R., Turmaine, M., Mangiarini, L., Hollenbach, B., Hasenbank, R., Bates, G. P., Davies, S. W., Lehrach, H., and Wanker, E. E. (1997) *Cell* **90,** 549–558
3. Michalik, A., and Van Broeckhoven, C. (2003) *Hum. Mol. Genet.* **12,** R173–R186
4. Yamamoto, A., Lucas, J. J., and Hen, R. (2000) *Cell* **101,** 57–66
5. Katsuno, M., Adachi, H., Doyu, M., Minamiyama, M., Sang, C., Kobayashi, Y., Inukai, A., and Sobue, G. (2003) *Nat. Med.* **9,** 768–773
6. Tanaka, M., Machida, Y., Niu, S., Ikeda, T., Jana, N. R., Doi, H., Kurosawa, M., Nekooki, M., and Nukina, N. (2004) *Nat. Med.* **10,** 148–154
7. Schilling, G., Savonenko, A. V., Klevytska, A., Morton, J. L., Tucker, S. M., Poirier, M., Gale, A., Chan, N., Gonzales, V., Slunt, H. H., Coonfield, M. L., Jenkins, N. A., Copeland, N. G., Ross, C. A., and Borchelt, D. R. (2004) *Hum. Mol. Genet.* **13,** 1599–1610
8. Jana, N. R., Tanaka, M., Wang, G., and Nukina, N. (2000) *Hum. Mol. Genet.* **9,** 2009–2018
9. Mitsui, K., Nakayama, H., Akagi, T., Nekooki, M., Ohtawa, K., Takio, K., Hashikawa, T., and Nukina, N. (2002) *J. Neurosci.* **22,** 9267–9277
10. Shimohata, T., Nakajima, T., Yamada, M., Uchida, C., Onodera, O., Naruse, S., Kimura, T., Koide, R., Nozaki, K., Sano, Y., Ishiguro, H., Sakoe, K., Ooshima, T., Sato, A., Ikeuchi, T., Oyake, M., Sato, T., Aoyagi, Y., Hozumi, I., Nagatsu, T., Takiyama, Y., Nishizawa, M., Goto, J., Kanazawa, I., Davidson, I., Tanese, N., Takahashi, H., and Tsuji, S. (2000) *Nat. Genet.* **26,** 29–36
11. Nucifora, F. C., Jr., Sasaki, M., Peters, M. F., Huang, H., Cooper, J. K., Yamada, M., Takahashi, H., Tsuji, S., Troncoso, J., Dawson, V. L., Dawson, T. M., and Ross, C. A. (2001) *Science* **291,** 2423–2428
12. Dunah, A. W., Jeong, H., Griffin, A., Kim, Y. M., Standaert, D. G., Hersch, S. M., Mouradian, M. M., Young, A. B., Tanese, N., and Krainc, D. (2002) *Science* **296,** 2238–2243
13. Chai, Y., Koppenhafer, S. L., Shoesmith, S. J., Perez, M. K., and Paulson, H. L. (1999) *Hum. Mol. Genet.* **8,** 673–682
14. Jana, N. R., Zemskov, E. A., Wang, G., and Nukina, N. (2001) *Hum. Mol. Genet.* **10,** 1049–1059
15. Doi, H., Mitsui, K., Kurosawa, M., Machida, Y., Kuroiwa, Y., and Nukina,

N. (2004) *FEBS Lett.* **571,** 171–176
16. Crozat, A., Aman, P., Mandahl, N., and Ron, D. (1993) *Nature* **363,** 640–644
17. Rabbitts, T. H., Forster, A., Larson, R., and Nathan, P. (1993) *Nat. Genet.* **4,** 175–180
18. Wang, G. H., Mitsui, K., Kotliarova, S., Yamashita, A., Nagao, Y., Tokuhiro, S., Iwatsubo, T., Kanazawa, I., and Nukina, N. (1999) *Neuroreport.* **10,** 2435–2438
19. Zemskov, E. A., Jana, N. R., Kurosawa, M., Miyazaki, H., Sakamoto, N., Nekooki, M., and Nukina, N. (2003) *J. Neurochem.* **87,** 395–406
20. Mitsui, K., Doi, H., and Nukina, N. (2006) *Methods Enzymol.* **412,** 63–76
21. Dignam, J. D., Lebovitz, R. M., and Roeder, R. G. (1983) *Nucleic Acids Res.* **11,** 1475–1489
22. Vonsattel, J. P., Myers, R. H., Stevens, T. J., Ferrante, R. J., Bird, E. D., and Richardson, E. P., Jr. (1985) *J. Neuropathol. Exp. Neurol.* **44,** 559–577
23. Oyama, F., Miyazaki, H., Sakamoto, N., Becquet, C., Machida, Y., Kaneko, K., Uchikawa, C., Suzuki, T., Kurosawa, M., Ikeda, T., Tamaoka, A., Sakurai, T., and Nukina, N. (2006) *J. Neurochem.* **98,** 518–529
24. Chien, P., DePace, A. H., Collins, S. R., and Weissman, J. S. (2003) *Nature* **424,** 948–951
25. Tanaka, M., Machida, Y., Nishikawa, Y., Akagi, T., Hashikawa, T., Fujisawa, T., and Nukina, N. (2003) *J. Biol. Chem.* **278,** 34717–34724
26. Zinszner, H., Sok, J., Immanuel, D., Yin, Y., and Ron, D. (1997) *J. Cell Sci.* **110,** 1741–1750
27. Davies, S. W., Turmaine, M., Cozens, B. A., DiFiglia, M., Sharp, A. H., Ross, C. A., Scherzinger, E., Wanker, E. E., Mangiarini, L., and Bates, G. P. (1997) *Cell* **90,** 537–548
28. Schaffar, G., Breuer, P., Boteva, R., Behrends, C., Tzvetkov, N., Strippel, N., Sakahira, H., Siegers, K., Hayer-Hartl, M., and Hartl, F. U. (2004) *Mol. Cell* **15,** 95–105
29. Derkatch, I. L., Uptain, S. M., Outeiro, T. F., Krishnan, R., Lindquist, S. L., and Liebman, S. W. (2004) *Proc. Natl. Acad. Sci. U. S. A.* **101,** 12934–12939
30. Serio, T. R., Cashikar, A. G., Kowal, A. S., Sawicki, G. J., Moslehi, J. J., Serpell, L., Arnsdorf, M. F., and Lindquist, S. L. (2000) *Science* **289,** 1317–1321
31. Perez, M. K., Paulson, H. L., Pendse, S. J., Saionz, S. J., Bonini, N. M., and Pittman, R. N. (1998) *J. Cell Biol.* **143,** 1457–1470
32. Kazantsev, A., Preisinger, E., Dranovsky, A., Goldgaber, D., and Housman, D. (1999) *Proc. Natl. Acad. Sci. U. S. A.* **96,** 11404–11409
33. Li, X. J., Li, S. H., Sharp, A. H., Nucifora, F. C., Jr., Schilling, G., Lanahan, A., Worley, P., Snyder, S. H., and Ross, C. A. (1995) *Nature* **378,** 398–402
34. Kegel, K. B., Meloni, A. R., Yi, Y., Kim, Y. J., Doyle, E., Cuiffo, B. G., Sapp, E., Wang, Y., Qin, Z. H., Chen, J. D., Nevins, J. R., Aronin, N., and DiFiglia, M. (2002) *J. Biol. Chem.* **277,** 7466–7476
35. Ross, C. A., and Poirier, M. A. (2004) *Nat. Med.* **10,** (suppl.) S10–S17
36. Nagai, Y., Inui, T., Popiel, H. A., Fujikake, N., Hasegawa, K., Urade, Y., Goto, Y., Naiki, H., and Toda, T. (2007) *Nat. Struct. Mol. Biol.* **14,** 332–340
37. Bucciantini, M., Giannoni, E., Chiti, F., Baroni, F., Formigli, L., Zurdo, J., Taddei, N., Ramponi, G., Dobson, C. M., and Stefani, M. (2002) *Nature* **416,** 507–511
38. Sanchez, I., Mahlke, C., and Yuan, J. (2003) *Nature* **421,** 373–379
39. Nagai, Y., Fujikake, N., Ohno, K., Higashiyama, H., Popiel, H. A., Rahadian, J., Yamaguchi, M., Strittmatter, W. J., Burke, J. R., and Toda, T. (2003) *Hum. Mol. Genet.* **12,** 1253–1259
40. Bertolotti, A., Lutz, Y., Heard, D. J., Chambon, P., and Tora, L. (1996) *EMBO J.* **15,** 5022–5031
41. Delva, L., Gallais, I., Guillouf, C., Denis, N., Orvain, C., and Moreau-Gachelin, F. (2004) *Oncogene* **23,** 4389–4399
42. Yang, L., Embree, L. J., Tsai, S., and Hickstein, D. D. (1998) *J. Biol. Chem.* **273,** 27761–27764
43. Kanai, Y., Dohmae, N., and Hirokawa, N. (2004) *Neuron* **43,** 513–525
44. Fujii, R., and Takumi, T. (2005) *J. Cell Sci.* **118,** 5755–5765
45. Fujii, R., Okabe, S., Urushido, T., Inoue, K., Yoshimura, A., Tachibana, T., Nishikawa, T., Hicks, G. G., and Takumi, T. (2005) *Curr. Biol.* **15,** 587–593
46. Klapstein, G. J., Fisher, R. S., Zanjani, H., Cepeda, C., Jokel, E. S., Chesselet, M. F., and Levine, M. S. (2001) *J. Neurophysiol.* **86,** 2667–2677
47. Ferrante, R. J., Kowall, N. W., and Richardson, E. P., Jr. (1991) *J. Neurosci.* **11,** 3877–3887
48. Kuhn, A., Goldstein, D. R., Hodges, A., Strand, A. D., Sengstag, T., Kooperberg, C., Becanovic, K., Pouladi, M. A., Sathasivam, K., Cha, J. H., Hannan, A. J., Hayden, M. R., Leavitt, B. R., Dunnett, S. B., Ferrante, R. J., Albin, R., Shelbourne, P., Delorenzi, M., Augood, S. J., Faull, R. L., Olson, J. M., Bates, G. P., Jones, L., and Luthi-Carter, R. (2007) *Hum. Mol. Genet.* **16,** 1845–1861